Motional effects in dynamics of fluorescence of cold atomic ensembles excited by resonance pulse radiation

A. S. Kuraptsev* and I. M. Sokolov†

Department of Fundamental Physical Research, Peter the Great St. Petersburg Polytechnic University, 195251 St. Petersburg, Russia

(Received 27 April 2023; accepted 31 August 2023; published 20 September 2023)

We report the investigation of the influence of atomic motion on the fluorescence dynamics of a dilute atomic ensemble driven by resonance pulse radiation. We show that even for sub-Doppler temperatures, the motion of atoms can significantly affect the nature of both superradiation and subradiation. We also demonstrate that, in the case of an ensemble of moving scatterers, it is possible to observe the nonmonotonic time dependence of the fluorescence rate. This leads to the fact that, in certain time intervals, increasing temperature causes not an decrease but an increase of the fluorescence intensity in the cone of coherent scattering. We analyze the role of the frequency diffusion of secondary radiation as a result of multiple light scattering in an optically dense medium. It is shown that spectrum broadening is the main factor which determines radiation trapping upon resonant excitation. Along with broadening, we found a shift and distortion of the shape of the spectrum over time. At later time, after the trapping stage, the dynamics is dominated by close pairs of atoms (dimers). The dynamics of the excited states of these dimers has been studied in detail. It is shown that the change in the lifetime of the given adiabatic term of the diatomic quasimolecule induced by the change in the interatomic distance as well as possible nonadiabatic transitions between sub- and superradiant states caused by atomic motion can lead not to the anticipated weakening of subradiation effect, but to its enhancement.

DOI: 10.1103/PhysRevA.108.032814

I. INTRODUCTION

Atomic ensembles cooled to sub-Doppler temperatures in special traps are currently of great interest both because of their number of unique physical properties and because of the wide range of their possible practical applications in problems of quantum metrology, frequency standardization, and quantum information applications [1–3].

Almost all proposed schemes for the use of cold atomic ensembles as well as most diagnostic methods are based on the interaction of these ensembles with electromagnetic radiation. This interaction has a number of features associated with collective polyatomic effects. These effects are due, first, to the large resonant cross sections for light scattering by each separate atom and, consequently, to the large optical depth of the ensembles even at low atomic densities. The second reason is random spatial disorder, in which the formation of atomic clusters, or quasimolecules, consisting of several atoms randomly located at distances of the order of the resonance radiation wavelength from each other is possible. Dipole-dipole interatomic interaction causes the formation of collective sub- and superradiant states, which can essentially affect the optical properties of cold gases.

Nowadays, the main approach to the description of collective effects is the so-called method of coupled oscillators. To date, several variants of this method have been developed [4–21]. The main difficulty in using this method is accounting for the motion of atoms in real physical systems. Therefore, in the overwhelming majority of works, the approximation of fixed scatterers is used. The displacement of atoms is taken into account by averaging the observables over a random spatial distribution of atoms. In Refs. [22–24] an attempt was made to refine the immobile atom approximation. In the refined model, the Doppler shift was modeled by introducing a random shift in the frequencies of atomic transitions, which is different for different atoms.

The effect of continuous displacement of atoms in dilute media was considered in the framework of the scalar approximation in [25]. A more detailed experimental and theoretical analysis was given in [26]. The main result of that work was the assertion that subradiative states are sufficiently resistant to thermal decoherence at the temperatures of the magneto-optical trap (MOT). Similar stability is predicted up to temperatures on the order of millikelvin. We came to a different conclusion in our group when considering dense atomic ensembles with a strong dipole-dipole interatomic interaction [27]. For clouds in which the average interatomic distance is comparable with the wavelength of resonant radiation, we observed the destruction of subradiative states even at temperatures several times lower than the typical MOT temperatures.

The essential influence of motion on another collective effect, the effect of single-photon superradiance, was discovered in the framework of the study of the flash effect in Refs. [28–30]. There, in particular, it was shown that the subradiation rate in the direction of the exciting pulse increases upon heating. For a flat layer of atoms for an infinitesimal time interval after the end of the excitation pulse, it was even possible to obtain analytical expressions confirming this growth. At

*aleksej-kurapcev@yandex.ru
†sokolov_im@spbstu.ru

the same time, theoretical studies of superradiance outside the cone of coherent forward scattering, carried out in [31], led to opposite conclusions. Heating manifests itself in a negative way, weakening the superradiance in these directions.

Thus, the available data indicate the complex nature of the influence of atomic motion on collective optical effects. This influence depends both on the nature of the effect and on the conditions of observation. The main goal of this work is a detailed study of dilute atomic ensembles cooled to sub-Doppler temperatures and excited by resonance pulsed radiation. Previously, the influence of motion on the character of radiative transfer, as well as the effects of sub- and superradiation under such conditions, was studied using the diagram technique (see the review in [32] and references therein) or using the transport equations [33] obtained on the basis of the generalized Bethe-Salpeter equations. In this work, we use a consistent microscopic approach that allows us to take into account many aspects that were not taken into account earlier and at the same time noticeably affect the phenomena under study. In particular, this approach makes it possible to account for the interatomic dipole-dipole interaction, as well as coherent effects such as interference and diffraction, which lead to a deviation from the Bouguer-Beer-Lambert law and cause weak localization effects. Within the framework of this unified approach, we will describe atomic fluorescence at various temperatures and over a wide time interval, including subradiance, light trapping, and single-photon superradiance. We will show that even when the characteristic Doppler frequency shifts are smaller than the natural width of atomic transitions, motion can significantly affect the fluorescence dynamics.

II. BASIC ASSUMPTIONS AND APPROACH

In our theoretical description of time-dependent fluorescence we use the coupled-dipole model, which is traditional for this class of problems [4–20].

We consider a disordered atomic ensemble of N identical two-level atoms. All atoms have a ground state $|g\rangle$ with total angular momentum $J_g = 0$, an excited state $|e\rangle$ with $J_e = 1$, and a transition frequency ω_0, and the natural lifetime of all excited Zeeman sublevels ($m = -1, 0, 1$) is $\tau_0 = 1/\gamma$.

Our specific calculations are based on an approach developed earlier in [12,27]. In accordance with this approach we study the properties of a closed system consisting of all atoms and an electromagnetic field, including a vacuum reservoir. We seek the wave function ψ of this system as an expansion over the eigenfunctions ψ_l of the Hamiltonian of noninteracting atoms and light $\psi = \sum_l \beta_l \psi_l$. Assuming that the exciting radiation is weak, which is typical in experiments [21,34,35], we take into account only states with no more than one photon in the field. In such a case for the amplitudes β_e of onefold excited atomic states $\psi_e = |g \cdots e \cdots g\rangle$ we have the following differential equation:

$$\frac{\partial \beta_e}{\partial t} = \left(i\delta - \frac{\gamma}{2}\right)\beta_e - \frac{i\Omega_e}{2} + \frac{i\gamma}{2}\sum_{e' \neq e} V_{ee'}\beta_{e'}. \tag{1}$$

Here, the index e shows both the number of the atom which is excited in state $\psi_e = |g \cdots e \cdots g\rangle$ and the specific Zeeman sublevel populated in this state; Ω_e is the Rabi frequency of the external laser field at the point where atom e locates, and δ is the detuning of the field from the resonance atomic frequency.

The last term in Eq. (1) corresponds to dipole-dipole interatomic interaction and is responsible for collective effects in the considered atomic ensemble. The matrix $V_{ee'}$ is

$$V_{ee'} = -\frac{2}{\gamma}\sum_{\mu,\nu} \mathbf{d}^{\mu}_{eg}\mathbf{d}^{\nu}_{ge'}\frac{e^{ik_0 r_{ij}}}{\hbar r^3_{ij}} \times \left\{\delta_{\mu\nu}[1 - ik_0 r_{ij} - (k_0 r_{ij})^2] - \frac{\mathbf{r}^{\mu}_{ij}\mathbf{r}^{\nu}_{ij}}{r^2_{ij}}[3 - 3ik_0 r_{ij} - (k_0 r_{ij})^2]\right\}. \tag{2}$$

Here, we assume that in the e state atom i is excited and in the e' state atom j is excited; $\mathbf{d}_{eg}$ is the matrix element of the dipole moment operator for the transition $g \to e$, $\mathbf{r}_{ij} = \mathbf{r}_i - \mathbf{r}_j$, $r_{ij} = |\mathbf{r}_i - \mathbf{r}_j|$, and $k_0 = \omega_0/c$ is the wave number associated with the transition, with c being the vacuum speed of light. The indexes μ and ν denote projections of vectors on the axes of the reference frame.

Note that, despite the fact that system (1) was formally obtained in the single-excitation approximation, it has been repeatedly verified that it describes well the results of experiments with real atomic ensembles if nonlinear optical effects can be neglected. It is sufficient to require that the saturation parameter for the pump radiation be much less than unity. In real experiments devoted to studying such linear optics collective effects as super- and subradiance, this parameter usually does not exceed 0.04 (see, for example, the review in [21] and references therein)

From the values of $\beta_e(t)$ computed on the basis of Eq. (1) we can find the amplitudes of all other states which determine the wave function ψ (for more details, see [12]), which, in turn, gives us information about the properties of the secondary radiation as well as about the properties of the atomic ensemble. In particular, the intensity $I_\alpha(\mathbf{\Omega}, t)$ of the light-polarization component α that the atoms scatter in a unit solid angle around the direction of the wave vector $\mathbf{k}$ determined by radius vector $\mathbf{r}$ ($\mathbf{\Omega} = \theta, \varphi$) reads

$$I_\alpha(\mathbf{\Omega}, t) = \frac{c}{4\pi}\langle\psi|E^{(-)}_\alpha(\mathbf{r})E^{(+)}_\alpha(\mathbf{r})|\psi\rangle r^2 = \frac{c}{4\pi}\left|k_0^2\sum_e(\mathbf{u}^*_\alpha\mathbf{d}_{ge})\beta_e(t)\exp(-i\mathbf{k}\mathbf{r}_i)\right|^2. \tag{3}$$

Here, $E^{(\pm)}_\alpha(\mathbf{r})$ are the positive- and negative-frequency parts of the electric-field operator; $\mathbf{u}_\alpha$ is the unit polarization vector of the scattered light.

In this paper, while analyzing the role of atomic motion, we will not conduct a detailed study of the angular distribution of fluorescence. The main focus will be on the study of the influence of temperature on the dynamics of the total radiation of the ensemble. This value can be obtained by integrating expression (3) over the total solid angle and summing the contributions of the various polarization components. It can also be calculated on the basis of the law of energy conservation,

taking into account that the total radiation energy is equal to the decrease in the excitation energy of the atomic system; that is, it can be determined from the rate of decrease in the total population $P_{\rm ex}(t)$ of the excited states of all atoms. The latter can be found as follows:

$$P_{\rm ex}(t) = \sum_e |\beta_e(t)|^2. \tag{4}$$

In the next section, based on relations (1)–(4), we will calculate the rate of decay of the total radiation intensity of an ensemble of moving atoms at different temperatures. We will look for a nonstationary solution to Eq. (1), taking into account the displacement of atoms with time explicitly. We will consider the temperature ranges typical for MOTs and higher, at which the momenta of atoms are much greater than the momenta of a photon. For this reason and also taking into account the weakness of the excitation, we will not take into account the recoil effects and will describe the motion as a classical uniform and rectilinear motion, $\mathbf{r}_i = \mathbf{r}_{i0} + \mathbf{v}_i(t - t_0)$. In order not to take into account the departure of atoms from the considered volume and associated change in their densities, we will assume that the volume of the cloud is surrounded by imaginary surfaces which scatter the atoms elastically without modification of their internal states. To simplify we consider an ensemble having the shape of a cube with the edge equal to L.

The distribution of atoms at initial time $t = t_0$ is considered random, but spatially homogeneous on average. The atomic medium is optically dense but dilute. The density of atoms n in all calculations will be the same, $nk_0^{-3} = 0.005$. The average distance between atoms in this case exceeds the wavelength of quasiresonant radiation.

The velocities of the atoms at $t = t_0$ are also considered as random variables. All their projections v_μ are assumed to have a Maxwell distribution corresponding to temperature T,

$$f(v_\mu) = 1/\sqrt{\pi v_0^2}\exp\left(-v_\mu^2/v_0^2\right). \tag{5}$$

Here $v_0 = \sqrt{2kT/m}$ is the most probable velocity and m is the mass of the atom. This velocity and the wave number k_0 determine the Doppler broadening of the line (FWHM) $\Delta_D = 2\sqrt{\ln 2}k_0 v_0$. All fluorescence parameters calculated in this paper will be obtained by averaging over random variables $\mathbf{r}_{i0}$ and $\mathbf{v}_i$.

The radiation pulse that excites fluorescence will be considered rectangular; its carrier frequency is resonant with the transition in a free atom $\delta = 0$. For definiteness, we choose it to be right-circularly polarized.

III. RESULTS

As the main quantity characterizing the dynamics of the fluorescence, we will use the current (instantaneous) radiation delay time $\tau(t) = 1/\Gamma(t)$, where $\Gamma(t) = \frac{1}{I(t)}\frac{dI(t)}{dt}$ and $I(t)$ is the total intensity of the secondary radiation of the atomic ensemble, i.e., intensity summed over all directions and all polarizations. Note that in the linear optics regime, the quantities $\tau(t)$ and $\Gamma(t)$ do not depend on the Rabi frequency of the pump radiation. The dependence $\tau(t)$ after the end of the excitation pulse at different temperatures for the ensemble containing $N = 625$ atoms (resonance optical depth for motionless atoms is $b_0 \simeq 4.71$) is shown in Fig. 1. The pulse duration $\gamma T_p = 50$ was chosen from the condition that by the end of the pulse, the equilibrium population of the excited state in the atomic ensemble must be established.

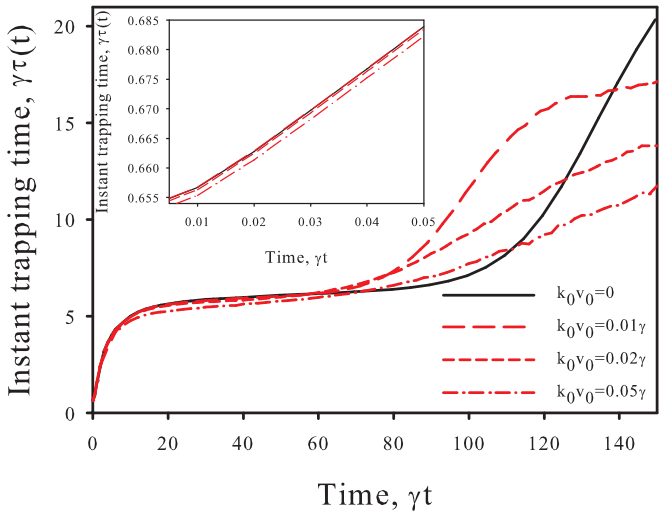

FIG. 1. Dynamics of instantaneous fluorescence delay time at various $k_0 v_0$ (temperatures). The number of atoms is $N = 625$; the resonance optical depth for motionless atoms is $b_0 \simeq 4.71$. The excitation pulse duration is $\gamma T_p = 50$. The time reference $t = 0$ corresponds to the end of the excitation pulse. Averaging is performed over at least 40 000 independent atomic configurations for each curve.

As for immobile atoms [36,37], several characteristic stages of fluorescence can be distinguished. First, at times $t < 1/\gamma$ after the end of the excitation pulse, the superradiance effect is observed. The dependence $\tau(t)$ at this stage is shown on an enlarged scale in the inset in Fig. 1. The decay rate $\Gamma(t)$ here is greater than the natural width γ, and $\gamma\tau(t) < 1$.

Then comes the stage of radiation trapping, which is caused by the diffusion of photons in an optically dense medium. It can be divided into two parts. Initially, the decay rate decreases, and the trapping time increases. Here, radiation diffusion is described by multimode dynamics. Further, the diffusion regime becomes single mode when the afterglow decay is described with good accuracy by a exponential law. This regime corresponds to rectilinear, almost horizontal segments on the $\tau(t)$ curves.

Finally, after this exponential phase, a noticeable increase in the trapping time $\tau(t)$ and a decrease in the decay rate are observed. Here, we are dealing with the radiation of clusters randomly formed in the considered disordered ensemble. These clusters have long-lived states that are responsible for the "classical" subradiation process predicted by Dicke [38].

Next, we consider in more detail those features of the fluorescence dynamics that result from taking into account the motion of atoms at each of these main stages.

A. Influence of motion on the nature of single-photon superradiance

As already mentioned, the effect of single-photon superradiance has been studied in sufficient detail. The dynamics of

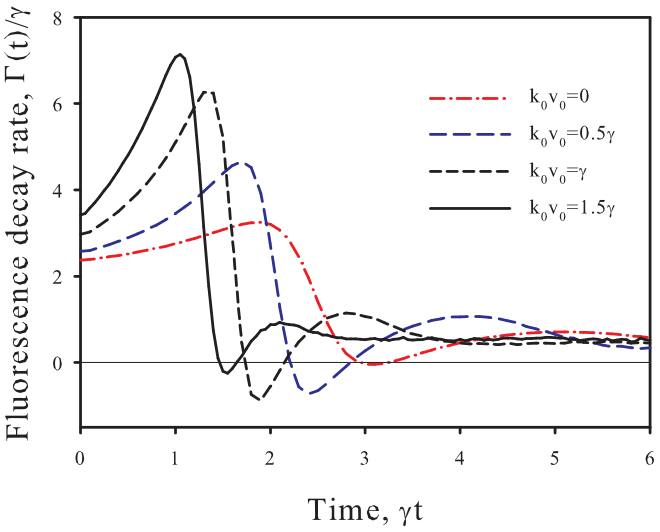

FIG. 2. Time dependence of the fluorescence rate in the forward direction $\Gamma(t)$ at different temperatures ($k_0 v_0$).

fluorescence in the cone of coherent forward scattering has especially been studied in detail. In particular, in an experiment [28] it was found that the rate of superradiance in this direction increases with heating. This unexpected effect was explained as the result of the dephasing effect from the motion of the atoms [30].

In the theoretical description of the flash effect, the most attention was paid to infinitesimal time intervals after the end of the excitation of atomic clouds having the form of a flat layer. This is the simplest case that admits an analytical description. In particular, for this case in [30] an explicit analytical expression for the superradiance velocity was obtained. For resonant excitation it reads as follows:

$$\Gamma(0^+) = \frac{b_0\gamma}{2\{1-\exp[-b(v_0)/2]\}}. \tag{6}$$

Here, $b(v_0)$ and b_0 are the optical thicknesses of the medium at a given temperature and at a temperature tending to zero, respectively.

In this work, we carry out a numerical analysis, which makes it possible to analyze the dynamics of the superradiance process in a wide time interval, taking into account the finite transverse dimensions of the ensemble. The results of this analysis for different temperatures are shown in Fig. 2.

The speed $\Gamma(t=0^+)$ immediately after the abrupt switching off of the excitation is qualitatively well described by Eq. (6). Some quantitative differences are due to the finite transverse size of the considered ensembles.

For $t>0$, on time intervals of the order of the natural lifetime of an atomic excited state the time dependence of $\Gamma(t)$ demonstrates some important features. For $t=0^+$, $\Gamma(t)$ is not maximal. After the excitation is turned off, $\Gamma(t)$ changes nonmonotonically. It can even change sign. That is, at certain time intervals, the intensity of secondary radiation in the coherent forward lobe does not decrease, but increases. The velocity Γ reaches its maximal negative values at $k_0 v_0 \sim \gamma$.

An oscillating behavior and a change in the sign of $\Gamma(t)$ can take place already for fixed atoms. We checked that in this case, these effects are stronger the greater the optical thickness b_0 is. At the same time for a given size of atomic cloud heating significantly enhances the considered effects, which is clearly seen in Fig. 2.

In our opinion the oscillation in the afterglow of the atomic ensemble is connected to quantum beating and is caused by interference of light scattering through different collective states [27,39].

To conclude this section, we note that for the flat-layer model, the time dependence of $G(t)$ can be analyzed within the framework of a computationally simpler approach used, for example, in [29,40]. The description of the dynamics can be carried out on the basis of a spectral analysis of stationary transmission using the Bouguer-Beer-Lambert law, followed by an inverse Fourier transform and transition to a time representation.

B. Influence of motion on diffusion trapping

It follows from Fig. 2 that, for the ensembles under study, the transient processes end at the time $\gamma t \sim 5$–6 after the superradiance stage. Then the trapping stage begins. Here, the trapping time changes slightly with temperature, which, in our opinion, is precisely what was observed in the experiment [26].

This result seems quite natural since, as is known, the diffusion trapping time τ_d, given by the horizontal segment in Fig. 1, is determined by the optical thickness b. For immobile atoms and clouds with large resonance optical thickness $b_0 = \sigma_0 nL \gg 1$ this time is well described by the following simple relation:

$$\tau_d = \frac{3b_0^2}{\alpha\pi^2}\tau_0, \tag{7}$$

where $\sigma_0 = 6\pi k_0^{-2}$ is the resonance cross section for the considered dilute media consisting of two-level atoms and the parameter α depends on the shape of the cloud. For cubic volume $\alpha = 3$.

The decrease in τ_d is associated with a change in the mean free path due to the Doppler effect. The role of this effect is relatively small at sub-Doppler temperatures. However, numerical calculations show that this decrease turns out to be more significant than relation (7) predicts if b_0 is replaced by $b(v) = b_0 g(k_0 v/\gamma)$ determined in accordance with the Voigt profile for moving atoms. Here, $g(x) = \sqrt{\pi/8}\exp(1/4x^2)\mathrm{erfc}(1/2x)/x$.

The solid line in Fig. 3 shows the calculated dependence of τ_d on the atomic velocity for an atomic ensemble with $k_0 L = 60$. The dashed line shows how the time τ_d would change if it were calculated using Eq. (7) while taking into account the dependence of the optical thickness on temperature. For the convenience of comparison, the results calculated using Eq. (7) were renormalized so that they coincided with the results of numerical calculations for immobile atoms. The need for renormalization is due to the limited applicability of Eq. (7) for a not very large optical depth of the atomic ensemble (see [41]).

Figure 3 demonstrates a noticeable discrepancy between the results of the two calculations, which can be explained by the photon frequency drift during multiple scattering

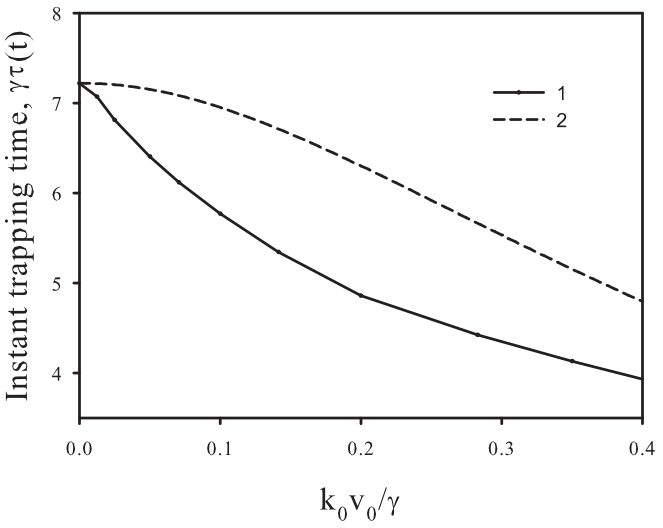

FIG. 3. Dependence of τ_d on $k_0 v_0$ (temperature) for an atomic ensemble with $k_0 L = 60$ ($b_0 \simeq 5.65$). The solid line gives the result of the numerical calculation. The dashed line is drawn on the basis of Eq. (7); $\gamma t = 40$.

inside the cloud [33,42,43]. In the multiple-scattering regime, a photon acquires a random frequency shift of the order of $k_0 v_0$ at each scattering, and its frequency performs a random walk in the frequency space. This frequency drift leads to the appearance of nonresonant photons, which have a large mean free path and, consequently, a shorter lifetime in the ensemble.

The broadening of the spectrum after the end of the excitation pulse under conditions close to those considered in this paper was investigated in [33]. There, the calculation was carried out based on the radiative transfer equation, which takes into account the motion of atoms. The results of our calculation performed using the coupled-oscillator method are shown in Fig. 4(a). The spectrum is calculated for radiation scattered at an angle of 90°. In contrast to [33], we use the short-term Fourier transform [44]. When analyzing the spectral composition of secondary radiation under essentially nonstationary conditions, this approach seems to us more natural than the usually determined time-dependent spectral intensity. The specific calculation was made for a rectangular window with duration $\gamma \Delta t = 30$. The center of the window was at different times γt after the end of the excitation pulse.

For illustration, in Fig. 4(b) we show the broadening of the spectrum upon heating for a fixed point in time. After the end of the excitation, the atoms begin to radiate at their own frequency. At times where the main mechanism is diffusion radiation trapping, there is a noticeable broadening of the spectrum due to multiple scattering. An increase in temperature (as well as an increase in the size of the cloud) enhances the effect of frequency drift, which explains the acceleration of fluorescence observed in Fig. 3.

C. Influence of motion on the subradiation of dimers

The role of motion manifests itself most unexpectedly at the stage of subradiation of diatomic clusters. As can be seen from Fig. 1, for all considered temperatures the motion reduces the duration of the trapping stage and also, at certain

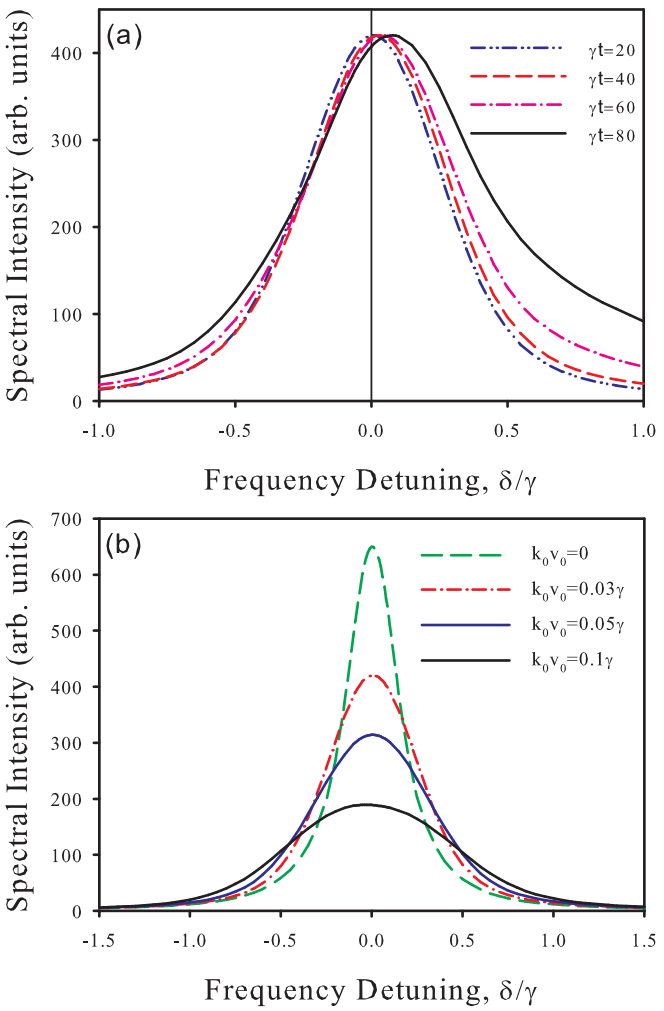

FIG. 4. Change in the shape of the fluorescence emission spectrum (a) over time at a fixed temperature $k_0 v_0 = 0.03\gamma$ and (b) during heating for a given moment of time $\gamma t = 20$. The ensemble size is $k_0 L = 50$. Averaging is performed over about 10 000 atomic configurations.

time intervals, leads not to a weakening, but to an increase in the subradiation effect.

The influence of dimers begins to dominate when the diffusion stage is completed. For the conditions for which Fig. 1 is drawn, this is the case for comparatively long times. The relative role of clusters can be enhanced if the diffusion effect is weakened. This can be done by reducing the optical thickness since the influence of dimers does not need to be revealed against the background of diffusion trapping.

This is well demonstrated in Fig. 5, which shows the dependence $\tau = \tau(t)$ for a fixed temperature corresponding to $k_0 v_0 = 0.02\gamma$ and a fixed atomic density $n k_0^{-3} = 0.005$ but for ensembles of different sizes with a small optical thickness.

Figure 5 shows another effect that appears when the motion is taken into account. For small systems, a nonmonotonic time dependence of the decay rate of the total fluorescence intensity is observed. At large times the curves $\tau = \tau(t)$ for ensembles of different sizes go to the same asymptote. This is because the characteristic lifetime of long-lived excited states of atomic

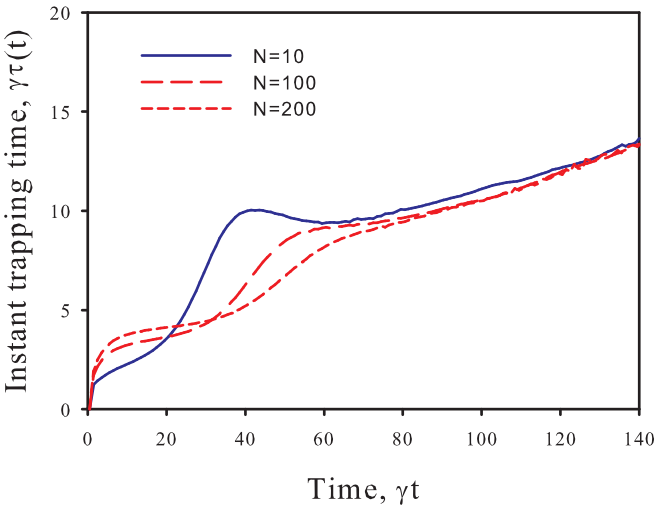

FIG. 5. Dynamics of instantaneous fluorescence delay time for various numbers of atoms. $k_0 v_0 = 0.2\gamma$; $nk_0^{-3} = 0.005$.

clusters depends on the average distance between atoms in them and does not depend on the size of the ensemble itself.

The main features of the influence of motion on cluster subradiation can be understood if we consider the temporal evolution of the excited state of a specific pair of atoms with a change in the distance between them. It is known that a system of two two-level atoms with $J_g = 0$ and $J_e = 1$ has six onefold excited collective states. These states can be calculated by diagonalizing the 6×6 matrix (3) for a diatomic system. Two pairs of states are degenerate. The frequency shifts Δ_c and the width Γ_c of the four distinct states of the stationary dimer can be found as follows:

$$\frac{\Delta_c}{\gamma} = \frac{3\epsilon}{4}\left[q\left(\frac{\cos(kr)}{(kr)^3} + \frac{\sin(kr)}{(kr)^2}\right) - \frac{p\cos(kr)}{kr}\right],$$

$$\frac{\Gamma_c}{\gamma} = 1 - \frac{3\epsilon}{2}\left[q\left(\frac{\sin(kr)}{(kr)^3} - \frac{\cos(kr)}{(kr)^2}\right) - \frac{p\sin(kr)}{kr}\right], \quad (8)$$

where $\epsilon = \pm 1$, $p_0 = 0$, $q_0 = -2$, $p_{\pm 1} = 1$, and $q_{\pm 1} = 1$.

Let us consider how the total intensity and the population of the excited state of a diatomic quasimolecule change with time if atoms move and the dimer is excited when the interatomic distance is equal to a given r_0.

Figure 6 shows the evolution of the considered system for two cases. Curves 1 and 2 correspond to the excitation of the longest-lived state and the shortest-lived one at r_0, respectively. For comparison curve 3 in Fig. 6(a) depicts the decay of noninteracting atoms at a rate of γ. The curves are calculated for $r_0 = 3.5k_0^{-1}$. The distance of closest approach is $r_m = 0.1k_0^{-1}$; the relative velocity of atoms is $k_0 v = 0.2\gamma$.

Note that for the chosen conditions, the initially short-lived state (curve 2) becomes subradiant upon approach. At small interatomic distances the population of the excited state practically does not change. The radiation intensity decreases significantly. This manifests itself as a dip in curve 2 in Fig. 6(b). After passing the point of closest approach, the radiation intensity increases. For the initial subradiant state, the picture is reversed. It decays very quickly when the atoms approach each other.

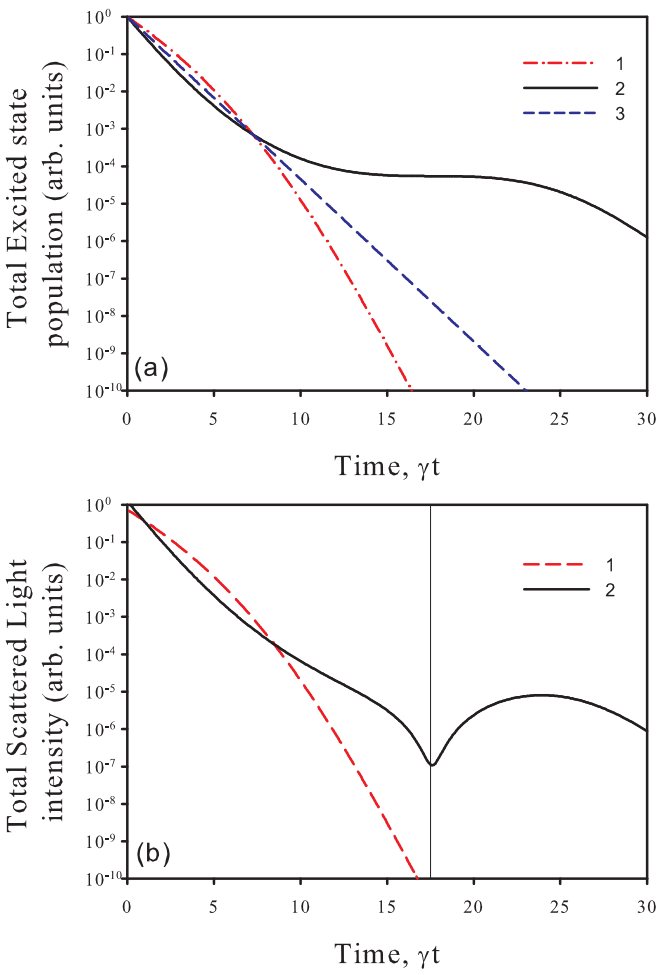

FIG. 6. (a) Dynamics of the population of the excited state of a diatomic quasimolecule with a change in the distance between atoms. (b) Time dependence of the total radiation intensity. Curve 1 corresponds to the initial excitation of the longest-lived state at $r_0 = 3.5k_0^{-1}$; curve 2 corresponds to the shortest-lived state. Curve 3 depicts the decay with a rate of γ. The relative velocity of atoms is $k_0 v = 0.2\gamma$. The distance of closest approach is $r_m = 0.1k_0^{-1}$. The vertical line corresponds to the moment of closest approach of the atoms.

For motionless atoms each eigenstate of a quasimolecule decays independently of the others. Therefore, when any one of them is excited, other states are not populated during the further evolution of the system. The subradiant state remains subradiative. This is not the case for moving atoms. The relation (8) describes the possibility of a subradiant state becoming superradiant even in the absence of transitions between different collective states. The decay rate of this state, i.e., of a state with given ϵ, p, and q, varies nonmonotonically with r and can be either greater or less than γ. This means that a change in the fluorescence rate of a cluster can be observed even in the absence of nonadiabatic transitions between its different states.

When atoms move, transitions between different collective states are also possible, which have an additional effect on the radiation dynamics. Such transitions are shown in Fig. 7. Here, we show the relative populations of four distinct states

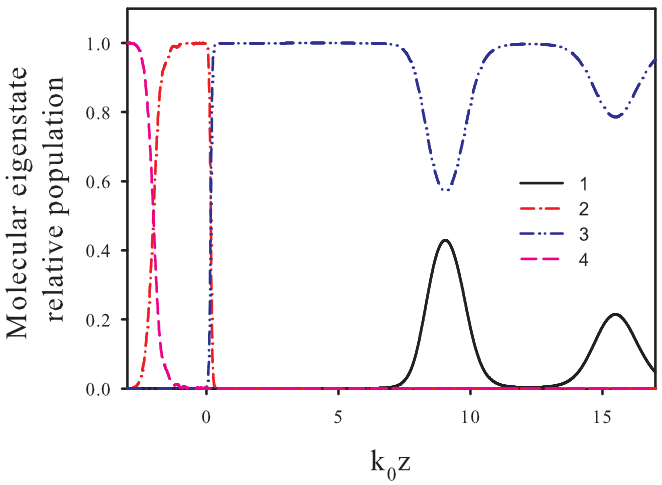

FIG. 7. Dynamics of the relative population of various collective states of a diatomic quasimolecule with a change in the distance between atoms. One of the atoms is stationary; the second one moves with speed $k_0 v = 0.05\gamma$ parallel to the z axis. Curve 1 corresponds to $\epsilon = 1$, $p = 1$, and $q = 1$; curve 2 corresponds to $\epsilon = -1$, $p = 1$, and $q = 1$; curve 3 corresponds to $\epsilon = -1$, $p = 0$, and $q = 2$; and curve 4 corresponds to $\epsilon = 1$, $p = 0$, and $q = 2$.

for different geometries of a diatomic quasimolecule. It is assumed that one of the atoms is immobile. It is located at the origin of coordinates. The second atom moves parallel to the z axis. At the initial moment of time, it was at the point $k_0 z_0 = -3, k_0 x_0 = 1,\ k_0 y_0 = 0$. At this moment, the system is excited to the state whose shift and width are given by formula (8) with $\epsilon = 1,\ p = 0$, and $q = 2$. Atom speed is equal to $k_0 v = 0.05\gamma$.

The transitions between different eigenstates of a diatomic quasimolecule are clearly visible. Note that for the parameters under consideration, after the scattering of atoms, the most populated state is the longest lived one with $\epsilon = -1$, $p = 0$, and $q = 2$. We checked that the last result is preserved regardless of which state was excited before the interatomic approach.

In a real multiatomic cloud, laser radiation excites not one, but a superposition of all possible states. And the nature of subradiation is determined by those that are subradiative at small interatomic distances. The others states decay rapidly, and their population turns out to be low, which is manifested in the fluorescence of the ensemble as a whole.

IV. CONCLUSION

In the present work, we studied the effect of atomic motion on the dynamics of the fluorescence of dilute atomic ensembles excited by resonant pulsed radiation. This effect was analyzed for three main stages of fluorescence evolution: the stage of superradiance, the stage of diffuse trapping of radiation, and the stage when subradiance is determined by the emission of atomic clusters randomly formed in the considered disordered atomic medium. It was shown that already for ensembles cooled to sub-Doppler temperatures, motion can significantly affect the nature of the considered collective effects.

It was found that, in addition to an increase in the subradiation velocity into the coherent forward-scattering cone, heating leads to the appearance of a nonmonotonic dependence of the radiation velocity. At certain time intervals, the decay of fluorescence in this direction can be replaced by its increase. At the trapping stage, the main factor affecting the fluorescence rate is the diffusion of the secondary radiation frequency as a result of multiple scattering of light in an optically dense medium. We studied the fluorescence spectrum and revealed its significant broadening upon heating of the ensemble. The most interesting results were found for subradiation of diatomic quasimolecules. In the temperature range corresponding to the MOT, the subradiation effect is enhanced for moving atoms. This effect is explained by the action of two factors, first, a change in the rate of decay of each of the eigenstates of a quasimolecule with a change in the distance between atoms and, second, possible nonadiabatic transitions between different sub- and superradiant states due to the motion of atoms.

ACKNOWLEDGMENTS

This research was supported by Grant No. 21-1-1-36-1 from the Foundation for the Development of Theoretical Physics and Mathematics "BASIS." Analysis of the broadening of the spectrum of secondary radiation was supported by the Russian Science Foundation (Grant No. 21-72-10004). The results of this work were obtained using the computing resources of the supercomputer center of Peter the Great St. Petersburg Polytechnic University.

[1] L. V. Hau, Nat. Photonics **2**, 451 (2008).
[2] D. Bouwmeester, A. Ekert, and A. Zeilinger, *The Physics of Quantum Information* (Springer, Berlin, 2010).
[3] B. J. Bloom, T. L. Nicholson, J. R. Williams, S. L. Campbell, M. Bishof, X. Zhang, W. Zhang, S. L. Bromley, and J. Ye, Nature (London) **506**, 71 (2014).
[4] L. L. Foldy, Phys. Rev. **67**, 107 (1945).
[5] M. Lax, Rev. Mod. Phys. **23**, 287 (1951).
[6] J. Javanainen, J. Ruostekoski, B. Vestergaard, and M. R. Francis, Phys. Rev. A **59**, 649 (1999).
[7] M. Rusek, J. Mostowski, and A. Orlowski, Phys. Rev. A **61**, 022704 (2000).
[8] F. A. Pinheiro, M. Rusek, A. Orlowski, and B. A. van Tiggelen, Phys. Rev. E **69**, 026605 (2004).
[9] H. Fu and P. R. Berman, Phys. Rev. A **72**, 022104 (2005).
[10] A. A. Svidzinsky, J.-T. Chang, and M. O. Scully, Phys. Rev. A **81**, 053821 (2010).
[11] D. V. Kuznetsov, Vl. K. Rerikh, and M. G. Gladush, J. Exp. Theor. Phys. **113**, 647 (2011).
[12] I. M. Sokolov, D. V. Kupriyanov, and M. D. Havey, J. Exp. Theor. Phys. **112**, 246 (2011).
[13] T. Bienaimé, R. Bachelard, P. W. Courteille, N. Piovella, and R. Kaiser, Fortschr. Phys. **61**, 377 (2013).

[14] S. E. Skipetrov and I. M. Sokolov, Phys. Rev. Lett. **112**, 023905 (2014).
[15] L. Bellando, A. Gero, E. Akkermans, and R. Kaiser, Phys. Rev. A **90**, 063822 (2014).
[16] W. Guerin, M. O. Araújo, and R. Kaiser, Phys. Rev. Lett. **116**, 083601 (2016).
[17] A. S. Kuraptsev and I. M. Sokolov, Phys. Rev. A **94**, 022511 (2016).
[18] W. Guerin, M. T. Rouabah, and R. Kaiser, J. Mod. Opt. **64**, 895 (2017).
[19] A. S. Kuraptsev, I. M. Sokolov, and M. D. Havey, Phys. Rev. A **96**, 023830 (2017).
[20] S. E. Skipetrov and I. M. Sokolov, Phys. Rev. B **99**, 134201 (2019).
[21] W. Guerin, Adv. At. Mol. Opt. Phys. **72**, 253 (2023).
[22] J. Javanainen, J. Ruostekoski, Y. Li, and S.-M. Yoo, Phys. Rev. Lett. **112**, 113603 (2014).
[23] S. D. Jenkins, J. Ruostekoski, J. Javanainen, S. Jennewein, R. Bourgain, J. Pellegrino, Y. R. P. Sortais, and A. Browaeys, Phys. Rev. A **94**, 023842 (2016).
[24] L. Bromley, B. Zhu, M. Bishof, X. Zhang, T. Bothwell, J. Schachenmayer, T. L. Nicholson, R. Kaiser, S. F. Yelin, M. D. Lukin, A. M. Rey, and J. Ye, Nat. Commun. **7**, 11039 (2016).
[25] T. Bienaime, N. Piovella, and R. Kaiser, Phys. Rev. Lett. **108**, 123602 (2012).
[26] P. Weiss, A. Cipris, M. O. Araújo, R. Kaiser, and W. Guerin, Phys. Rev. A **100**, 033833 (2019).
[27] A. S. Kuraptsev and I. M. Sokolov, Phys. Rev. A **101**, 033602 (2020).
[28] M. Chalony, R. Pierrat, D. Delande, and D. Wilkowski, Phys. Rev. A **84**, 011401(R) (2011).
[29] C. C. Kwong, T. Yang, M. S. Pramod, K. Pandey, D. Delande, R. Pierrat, and D. Wilkowski, Phys. Rev. Lett. **113**, 223601 (2014).
[30] C. C. Kwong, T. Yang, D. Delande, R. Pierrat, and D. Wilkowski, Phys. Rev. Lett. **115**, 223601 (2015).
[31] P. Weiss, A. Cipris, R. Kaiser, I. M. Sokolov, and W. Guerin, Phys. Rev. A **103**, 023702 (2021).
[32] D. V. Kupriyanov, I. M. Sokolov, and M. D. Havey, Phys. Rep. **671**, 1 (2017).
[33] R. Pierrat, B. Grémaud, and D. Delande, Phys. Rev. A **80**, 013831 (2009).
[34] S. J. Roof, K. J. Kemp, M. D. Havey, and I. M. Sokolov, Phys. Rev. Lett. **117**, 073003 (2016).
[35] M. O. Araújo, I. Kresic, R. Kaiser, and W. Guerin, Phys. Rev. Lett. **117**, 073002 (2016).
[36] Y. A. Fofanov, I. M. Sokolov, R. Kaiser, and W. Guerin, Phys. Rev. A **104**, 023705 (2021).
[37] I. M. Sokolov, J. Exp. Theor. Phys. **132**, 56 (2021).
[38] R. H. Dicke, Phys. Rev. **93**, 99 (1954).
[39] R. Röhlsberger, K. Schlage, B. Sahoo, S. Couet, and R. Rüffer, Science **328**, 1248 (2010).
[40] V. M. Datsyuk, I. M. Sokolov, D. V. Kupriyanov, and M. D. Havey, Phys. Rev. A **74**, 043812 (2006).
[41] M. C. W. van Rossum and Th. M. Nieuwenhuizen, Rev. Mod. Phys. **71**, 313 (1999).
[42] G. Labeyrie, D. Delande, R. Kaiser, and C. Miniatura, Phys. Rev. Lett. **97**, 013004 (2006).
[43] S. E. Skipetrov, I. M. Sokolov, and M. D. Havey, Phys. Rev. A **94**, 013825 (2016)
[44] S. V. Bozhokin and I. M. Sokolov, Tech. Phys. **63**, 1711 (2018).